

T_c up to 50 K in superlattices of insulating oxides

**D Di Castro¹, C Aruta¹, A Tebano¹, D Innocenti¹, M Minola²,
M Moretti Sala^{2,3}, W Prellier⁴, O Lebedev⁴ and G Balestrino¹**

¹ CNR-SPIN and Dipartimento di Ingegneria Civile e Ingegneria Informatica, Università di Roma Tor Vergata, Via del Politecnico 1, I-00133 Roma, Italy

² CNISM and Dipartimento di Fisica, Politecnico di Milano, I-20133, Italy

³ European Synchrotron Radiation Facility, BP 220, F-38043 Grenoble Cedex, France

⁴ Laboratoire CRISMAT, UMR 6508, CNRS-ENSICAEN 6 Bd Marechal Juin, F-14050 Caen, France

E-mail: daniele.di.castro@uniroma2.it

Received 1 November 2013, revised 29 January 2014

Accepted for publication 11 February 2014

Published 18 March 2014

1. Introduction

Cuprate high transition temperature (T_c) superconductors are naturally layered systems, where charge reservoir (CR) blocks are alternated with blocks containing CuO_2 planes with an infinite layer (IL) structure. When the CR blocks are charge unbalanced by cation substitution or oxygen deficiency/excess, they provide mobile holes or electrons to the CuO_2 layers. The recent improvements of the layer by layer deposition techniques have allowed the growth of high quality oxide heterostructures with sharp interfaces. In particular, the opportunity to mimic the layered structure of cuprates superconductors has been exploited by synthesizing novel high T_c superconducting heterostructures based on insulating and non-superconducting metallic cuprates [1, 2]. T_c as high as 80 K was first found in $\text{CaCuO}_2/\text{BaCuO}_2$ superlattices [1]. Subsequently, other cuprate/cuprate heterostructures based on the

superconductivity shows up [4]. The superconductivity in this case is confined within a few unit cells at the interface, and the CR role is played by the interface itself, thanks to the extra oxygen ions which enter at the interfaces during the growth in highly oxidizing growth conditions [4, 5]. Here we show that the T_c is strongly dependent on the substrate used and that T_c as high as 50 K (larger than the previously obtained 40 K in [4]) can be achieved in $[(\text{CaCuO}_2)_n/(\text{SrTiO}_3)_m]_N$ superlattices. We also give additional evidence that the interfaces are of fundamental importance for the superconductivity in these systems.

2. Experimental details

We used the pulsed laser deposition (PLD) technique (KrF excimer laser = 248 nm) to synthesize several superlattice (SL) films $[(\text{CaCuO}_2)_n/(\text{SrTiO}_3)_m]_N$, made by $N = 10\text{--}20$ repetitions of the supercell $(\text{CaCuO}_2)_n/(\text{SrTiO}_3)_m$. Most of the films were deposited on $5 \times 5 \text{ mm}^2$ NdGaO₃ (110) (NGO) oriented mono-crystalline substrates. Indeed, NGO is the most suitable substrate to grow CCO [6] and has a pseudocubic in-plane lattice parameter ($a = 3.87 \text{ \AA}$) just in the middle between CCO ($a = 3.84 \text{ \AA}$) and STO ($a = 3.91 \text{ \AA}$). Two targets, with CaCuO₂ and SrTiO₃ nominal composition, mounted on a multitarget system, were used. The STO target is a commercial crystal obtained from CRYSTAL GmbH. The CCO target was prepared by standard solid state reaction, as described in [4]. The substrate was placed at a distance of about 2.5 cm from the targets on a heated holder and its temperature during the deposition of the SLs was $T \approx 600 \text{ }^\circ\text{C}$. For the growth of the superconducting SLs the deposition chamber was first evacuated down to $P \approx 10^{-5}$ mbar and then a mixture of oxygen and 12% ozone atmosphere at a pressure of about 1 mbar was used, followed by a rapid quenching in high oxygen pressure (about 1 bar). Non-superconducting SLs were grown at the same temperature and pressure but with no ozone and no high pressure quenching.

The transport properties of the films have been measured by using the four-probe dc technique in the van der Pauw geometry, so that the measured resistance R is given by $R = R_s \ln 2/\pi$, where R_s is the sheet resistance. Four small contacts were made by silver epoxy directly at the corners of the square substrate before the film deposition, in order to avoid any chemical reaction between the SL and the solvent utilized in the silver epoxy.

The structural properties of the films were determined by means of x-ray diffraction using a $\theta\text{--}2\theta$ Bragg–Brentano diffractometer with Cu $K\alpha$ radiation.

The x-ray absorption spectroscopy (XAS) experiment was performed at the beamline ID08 of the European Synchrotron Radiation Facility using the high scanning speed Dragon-type monochromator. The x-ray source was an Apple II undulator delivering almost 100% polarized radiation in both horizontal and vertical directions. The total electron yield detection had a probing depth of 3–6 nm, so that several superlattice cells under the surface could be investigated. The incident beam formed a 60° angle with the sample surface normal, which is parallel to the crystal c -axis. In this geometry, with vertical

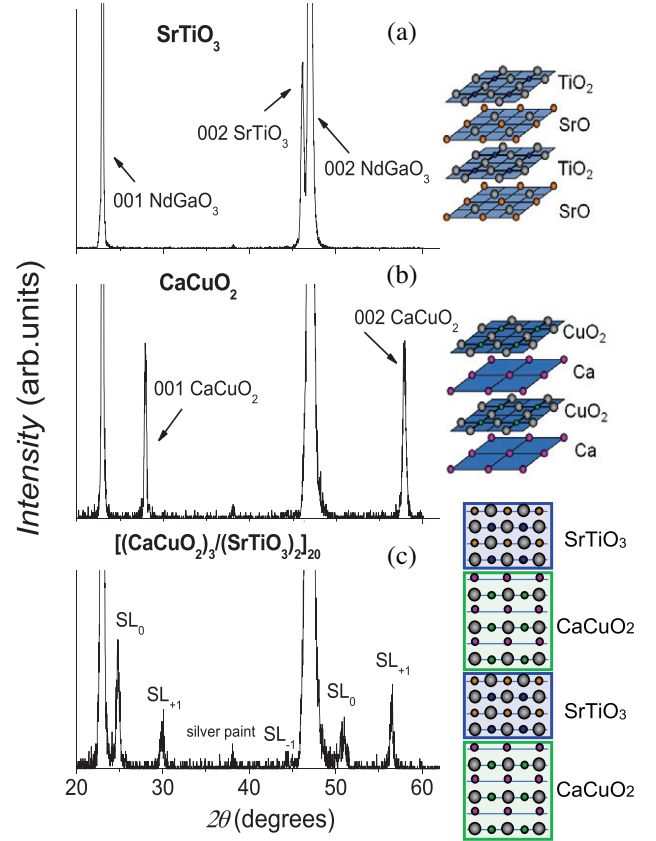


Figure 1. XRD spectra of CCO film (a), STO film (b) and CCO/STO superlattice (c) with the corresponding lattice structure.

polarization, the electric field vector \mathbf{E} of the incident radiation was parallel to the ab -plane. With horizontal polarization, \mathbf{E} was mostly parallel to the c -axis, so that 75% of the intensity comes from the final states lying perpendicular to the ab -plane.

3. Results and discussion

In figure 1, the XRD spectra of a CCO film, a STO film, and a $[(\text{CCO})_7/(\text{STO})_2]_{20}$ superlattice are shown. All three spectra indicate a good structural quality of the films grown, with absence of spurious phases. In the STO spectrum (figure 1(a)), only the (002) reflection is revealed, since the (001) one is hindered by the (001) reflection of NGO. The small peak at $2\theta \approx 38^\circ$ in all the spectra of figure 1 is due to the silver paint spots on the surface of the samples used for transport measurements. From the comparison of figures 1(a) and (b) with figure 1(c), it is clear that the spectrum of the SL is not just the sum of the CCO and STO spectra, but represents a new structural phase, confirming the occurrence of a superlattice structure, where SL_0 is the mean structure peak, and the $\text{SL}_{\pm i}$ are the satellite peaks.

To check the occurrence of a superlattice structure, we also made XRD measurements on a series of SLs $[(\text{CaCuO}_2)_n/(\text{SrTiO}_3)_2]$ with fixed number of STO unit cells, $m = 2$, and various numbers of CCO unit cells n ranging from 3 to 20. The spectra around the NGO substrate (001) reflection are shown in figure 2. The good quality of the superlattice structure

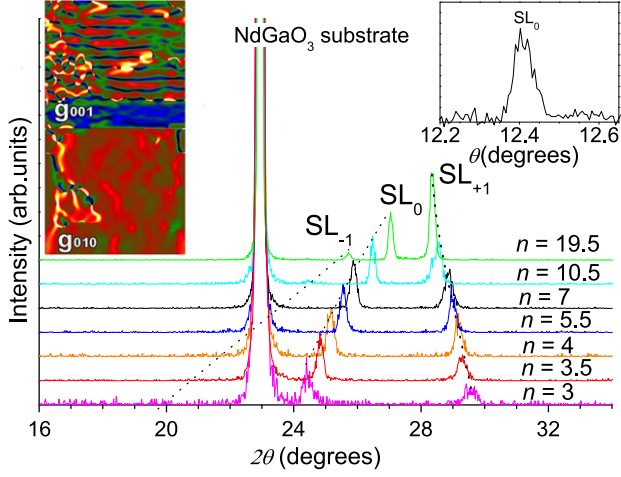


Figure 2. θ - 2θ scan around the (001) peak of the NdGaO₃ substrate on a sequence of SLs (CCO)_n/(STO)₂ where the number of STO unit cells is fixed at $m = 2$ and that of CCO is varied from $n = 3$ to $n = 20$. Right inset: rocking curve at the SL₀ peak of the $n = 3.5$ superlattice. Left inset: GPA image of (CCO)_{3.5}/(STO)₂ SL. Along the in-plane direction it is shown that both materials, CCO and STO, adopted the lattice parameters of NdGaO₃.

is clearly demonstrated by the presence of sharp superlattice satellite peaks SL_{-i} and SL_{+i} around the mean structure peak SL₀ and by their evolution with n . Indeed, since the c -axis parameter of the CCO (bulk value 3.19 Å) is smaller than that of STO (bulk value 3.91 Å), as the number of CCO unit cells increases, the SL₀ peak shifts towards higher 2θ values (smaller average c -axis parameter), while the distances of satellite peaks from SL₀ shrink because of the increased thickness of the supercell (CaCuO₂)_n/(SrTiO₃)₂. All films were found to have a very small value of the mosaic spread ($\approx 0.07^\circ$) very close to the substrate one ($\approx 0.06^\circ$) (see, as an example, the rocking curve of the (CaCuO₂)_{3.5}/(SrTiO₃)₂ superlattice in the inset of figure 2).

The overall experimental data collected up to now on CCO/STO SLs suggest the confinement of superconductivity within a few unit cells at the CaCuO₂/SrTiO₃ interface and the important role of additional oxygen atoms entering the interfaces during growth in an oxygen rich environment [4, 5, 7]. The excess oxygen atoms, most likely, lie in the Ca planes of CCO at the interface with the TiO₂ planes of STO (see schematic structure of CCO, STO and CCO/STO SLs in figure 1) and provide doping holes to the inner CuO₂ planes [4, 5]. Therefore, the interfaces in these SLs behave as a charge reservoir for the CuO₂ planes, allowing superconductivity in the CCO layer.

To further confirm the important role of the interfaces as the location where the doping and superconductivity occur, we made XAS measurements on the superconducting SL [(CCO)₁₃/(STO)₂]₁₈, with $m = 2$ u.c. of STO and $n = 13$ u.c. of CCO, to compare with the already measured superconducting SL [(CCO)₃/(STO)₂]₁₈, which has the same number of STO unit cells ($m = 2$) but thinner CCO ($n = 3$). The two samples were grown in identical oxidizing conditions in order to guarantee the same amount of extra oxygen and thus the same doping. XAS is a well established synchrotron based

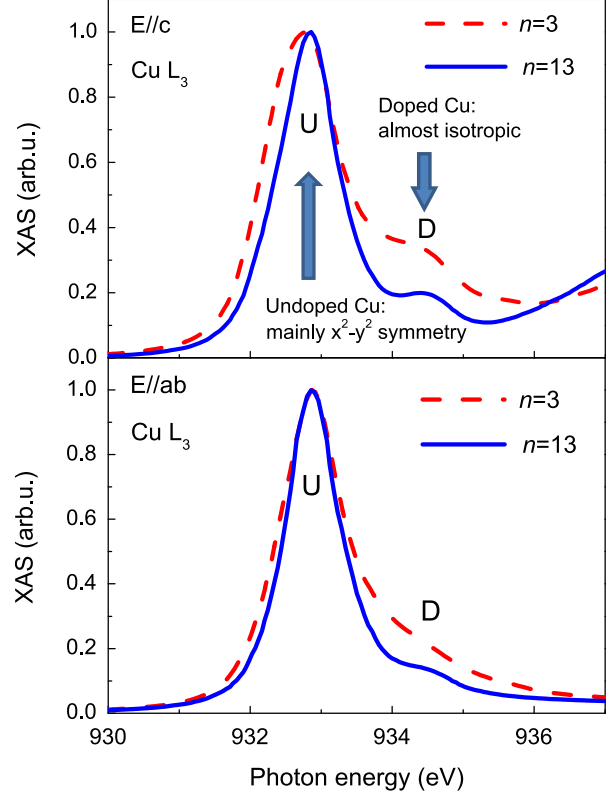


Figure 3. XAS spectra with $E \parallel c$ (upper panel) and $E \parallel ab$ (lower panel) of two superconducting superlattices: (CCO)₃/(STO)₂ (taken from [4]) and (CCO)₁₃/(STO)₂.

technique providing chemical and site selective information on the electronic states close to the Fermi level. In highly correlated 3d transition metal systems L_{2,3} edge XAS (mainly 2p → 3d transitions) can reveal the symmetry of unoccupied 3d states and distinguish among sites with different valences. We measured XAS at the Cu L₃ edges [8] at $T = 5$ K.

In figure 3 the normalized XAS spectra at the Cu L₃ edge with $E \parallel c$ (upper panel) and $E \parallel ab$ (lower panel) are shown for the two films. The Cu L₃ XAS main features, indicated with U and D in figure 3, have been associated, in analogy with the same measurements in cuprate high T_c superconductors [9, 10] and in other cuprate based superlattices [11], to the processes $3d^9 \rightarrow \underline{c}3d^{10}$ (U) and $3d^9\underline{L} \rightarrow \underline{c}3d^{10}\underline{L}$ (D), for the undoped and hole doped Cu sites, respectively, where \underline{c} indicates a Cu 2p core hole and \underline{L} indicates the oxygen ligand hole arising from Cu 3d-O 2p hole mainly with an O 2p character [4]. Indeed, as shown in [4], in both the polarizations the region around D acquires spectral weight in the case of superconducting SLs with respect to non-superconducting SLs grown in less oxidizing growth conditions. This finding clearly indicates the increased hole concentration in the O 2p bands and the presence of apical oxygen for the doped Cu sites. The comparison between the two superconducting SLs with different thicknesses of the CCO block shows that the intensity of the D peak, associated with the doped Cu sites, relative to the intensity of the U peak, associated with undoped Cu sites, substantially decreases with increasing n from 3 to 13. On the other hand, with increasing n , the

relative contribution to the XAS spectrum of the interface layers decreases. Thus, this result represents a spectroscopic confirmation of the importance of the interfaces in the doping process, and that the superconductivity is confined close to them.

Moreover, an increased spectral weight on the low energy side of the Cu L_3 absorption edge in the $E \parallel c$ spectrum is observed for the $n = 3$ superlattice, that is, when a higher density of interfaces is probed. In general, an energy shift in an XAS experiment is caused by changes in the electrostatic energy at the ion site, driven by a change in the effective ion charge. Therefore, a complex electronic reconstruction must be envisaged near the interfaces, provided that a lower attractive electrostatic energy at the *undoped* Cu site occurs. As reported in the paper of Chakhalian *et al* [12] for $\text{La}_{0.67}\text{Ca}_{0.33}\text{MnO}_3/\text{YBa}_2\text{Cu}_3\text{O}_7$ heterostructure, and confirmed in the case of $\text{La}_{0.7}\text{Sr}_{0.3}\text{MnO}_3/\text{CaCuO}_2$ [13], the presence of a Cu $3d_{z^2-r^2}$ orbital at the interface may give rise to a covalent chemical bond with the facing transition metal ion (Ti, in our case) via the p_z orbitals on the apical oxygen. Therefore, a substantial fraction of the negative charge density in the covalent bond resides on Cu, giving rise to spectral weight on the low energy side of the Cu L_3 absorption edge. Thus, apical oxygen is also present at the undoped Cu sites. Indeed, there are two kinds of interface in the superlattices, as it is possible to evince from the schematic representation of the SL in figure 1. In an ideal situation, the Cu ions can have apical oxygens only at the interface $\text{Ca}-\text{CuO}_2-\text{SrO}-\text{TiO}_2$, provided by the oxygen ions in the SrO planes, which, being stoichiometric, do not provide hole doping, whereas at the interface $\text{CuO}_2-\text{Ca}-\text{TiO}_2-\text{SrO}$, the Cu ions do not have apical oxygens. However, when the superlattice is grown in strongly oxidizing conditions, non-stoichiometric x oxygen ions enter at the $\text{CuO}_2-\text{CaO}_x-\text{TiO}_2-\text{SrO}$ interface in the Ca planes, providing hole doping. Therefore, the spectral weight on the low energy side of the Cu L_3 edge presumably derives from the undoped Cu site at the interface with the SrO plane of STO, whereas that on the high energy side (D) comes from the doped Cu sites at the other interface. This interpretation is also confirmed by the fact that the non-superconducting SL with $n = 3$ (see [4]) presents exactly the same low energy side behaviour of the superconducting SL with the same interface density ($n = 3$).

Since, as shown, the superconductivity in CCO/STO SLs is an interface phenomenon and it is obtained by the introduction of excess oxygen ions at the interface between CCO and STO, we tried to increase the oxidation of our films by adjusting the experimental growth setup. In particular, we have found that by correctly tuning the ozone flux into the growth chamber the T_c (zero resistance temperature) can be increased from 40 K [4] to 50 K (see figure 4). Indeed, the oxygen/ozone flow is generally delivered by a small tube (diameter 1 mm) positioned between the target and the substrate, in order that the plume coming from the target is well oxygenated before reaching the substrate. To improve the oxygenation, we moved the tube closer to the surface of the substrate. In this way, part of the flow also hits the substrate. In this situation, the amount of delivered flow is also

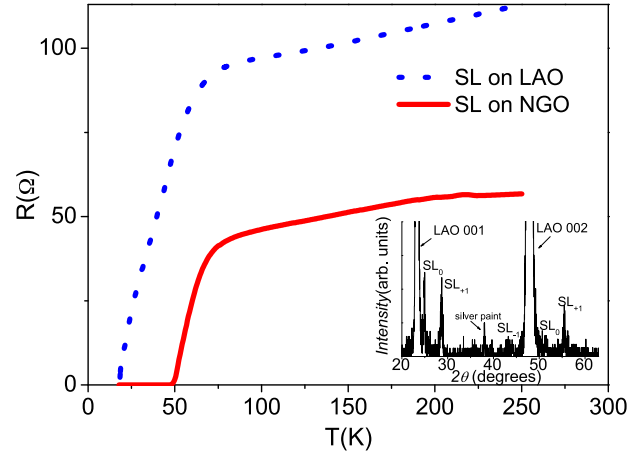


Figure 4. Temperature dependence of the resistance for the best superlattice grown on NGO (full line) and one superlattice grown on LAO (dashed line). Inset: XRD spectrum of the superlattice grown on LAO.

critical. A fine tuning, which depends on the geometry of the chamber, the base pressure reached before the introduction of the oxygen/ozone mixture, and the growth pressure, allowed an increase of T_c by 10 K. Therefore we deduced that, in this way, higher oxygenation is induced. The fact that a T_c larger than 40 K, which is about the maximum T_c for the electron doped cuprate superconductors and also for the family of hole doped cuprate superconductors $\text{La}_{(2-x)}\text{Sr}_x\text{CuO}_4$, has been reached suggests the possibility that T_c higher than 50 K could be obtained.

Another way to tune the T_c is the application of epitaxial strain throughout the substrate. Geometric phase analysis (GPA) [14] was performed to evaluate this strain on the same sample as used for the HRTEM image [4]. The GPA image (right up inset of figure 2) recorded along the out-of-plane direction ($g001$) shows that the CCO and STO layers have different lattice parameters along the film growth direction. The colour change between CCO and STO indicates that the out-of-plane lattice parameter of STO is larger than the NGO one, whereas that of CCO is smaller, as expected. On the other hand, along the in-plane direction of the substrate ($g010$), no difference in colour between the substrate, chosen as reference, and the superlattice layers is evidenced, indicating that both materials, CCO and STO, are strained within the in-plane direction and adopted the in-plane lattice parameters of the NdGaO_3 substrate. Therefore, by changing the substrate, this will affect a large fraction of the superlattice supercells. We have thus grown some superlattices on LaAlO_3 (LAO) substrate. As previously found in the samples used for a Raman study [15], the SLs grown on LAO show a much lower T_c than those grown on NGO. The $R(T)$ for a representative sample is shown in figure 4 together with the $R(T)$ curve of the optimal SL grown on NGO. The experimental observation that the quality of the XRD pattern, still being good (see inset of figure 4), is a little worse than that of SLs grown on NGO (lower intensity of the superlattice peaks, fewer superstructure orders shown, larger peak width) could in part explain this suppression of T_c , since we observed that high T_c and high structural quality (and thus sharpness of the interfaces) are

generally connected. However, other factors could be invoked. The effect of pressure on the T_c in cuprate superconductors has been widely studied [16–19] and it was found [20] that T_c increases with increasing in-plane uniaxial pressure, whereas it decreases with compression of the c -axis. Epitaxial strain thus has a substantial effect. For compressive strain, the in-plane lattice constant reduces, whereas the c -axis should increase because of the Poisson effect and thus an increase of T_c is expected. In contrast, tensile epitaxial strains should reduce T_c . However, in our superconducting cuprate/titanate superlattices, it seems that the effect of compressive epitaxial strain induces a decrease of T_c . Bozovic *et al* [21] observed that in $\text{La}_{(2-x)}\text{Sr}_x\text{CuO}_{4+\delta}$ films the great sensitivity to oxygen content, modified with the annealing processes, is the primary cause for the variations of T_c , rather than the epitaxial strain. Therefore, we think that in our SLs, which superconduct thanks to the extra oxygen atoms forced to the interfaces, the positive effect of in-plane lattice compression is overcome by the concomitant effects of the worse quality of the interfaces and the reduced space available for the extra oxygen ions. Both the latter effects could drastically reduce the number of extra oxygen ions within the active interfaces, thus reducing the hole doping and suppressing T_c .

4. Conclusions

We have reported a study of the recently discovered $\text{CaCuO}_2/\text{SrTiO}_3$ superconducting artificial superlattices. The XRD showed a good quality superlattice structure. The GPA analysis revealed that both CCO and STO in-plane lattice parameters are matched with those of the substrate. Thus, the use of LAO substrate, with lattice parameters substantially smaller than NGO, strongly affected the superlattice by inducing a compressive epitaxial strain. This caused a suppression of T_c , which turned out to be much lower than the maximum of 50 K found in superlattices grown on NGO under optimized growth conditions. The important role played by the interface layers has been demonstrated using x-ray absorption spectroscopy measurement as a function of the thickness of the CaCuO_2 block. This study confirmed that the hole doping and superconductivity are located close to the CCO/STO interfaces.

Acknowledgments

Partial support of the French Agence Nationale de la Recherche (ANR), through the program Investissements d’Avenir (ANR-10-LABX-09-01), LabEx EMC3 and the Interreg IVA MEET project is also acknowledged.

References

- [1] Balestrino G, Martellucci S, Medaglia P G, Paoletti A and Petrocelli G 1998 *Phys. Rev. B* **58** R8925
- [2] Gozar A, Logvenov G, Fitting Kourkoutis L, Bollinger A T, Giannuzzi L A, Muller D A and Bozovic I 2008 *Nature* **455** 782
- [3] Reyren N *et al* 2007 *Science* **317** 1196
- [4] Di Castro D *et al* 2012 *Phys. Rev. B* **86** 134524
- [5] Aruta C, Schlueter C, Lee T-L, Di Castro D, Innocenti D, Tebano A, Zegenhagen J and Balestrino G 2013 *Phys. Rev. B* **87** 155145
- [6] Balestrino G, Desfeux R, Martellucci S, Paoletti A, Petrocelli G, Tebano A, Mercey B and Hervieu M 1995 *J. Mater. Chem.* **5** 1879
- [7] Salvato M, Ottaviani I, Lucci M, Cirillo M, Di Castro D, Innocenti D, Tebano A and Balestrino G 2013 *J. Phys.: Condens. Matter* **25** 335702
- [8] de Groot F M F, Fuggle J C, Thole B T and Sawatzky G A 1990 *Phys. Rev. B* **41** 928
- [9] Bianconi A, Congiu Castellano A, De Santis M, Rudolf P, Lagarde P, Flank A M and Marcelli A 1987 *Solid State Commun.* **63** 1009
- [10] Sarma D D, Strebel O, Simmons C T, Neukirch U, Kaindl G, Hoppe R and Muller H P 1988 *Phys. Rev. B* **37** 9784
- [11] Aruta C, Ghiringhelli G, Dallera C, Fracassi F, Medaglia P G, Tebano A, Brookes N B, Braicovich L and Balestrino G 2008 *Phys. Rev. B* **78** 205120
- [12] Chakhalian J, Freeland J W, Habermeier H-U, Cristiani G, Khaliullin G, van Veenendaal M and Keimer B 2007 *Science* **318** 1114
- [13] Yang N *et al* 2012 *J. Appl. Phys.* **112** 123901
- [14] Hÿtch M J, Snoeck E and Kilaas R 1998 *Ultramicroscopy* **74** 131
- [15] Di Castro D, Caramazza S, Innocenti D, Balestrino G, Marini C, Dore P and Postorino P 2013 *Appl. Phys. Lett.* **103** 191903
- [16] Wijngaarden R J and Griessen R 1989 *Studies of High Temperature Superconductors* vol 2, ed A V Narlikar (New York: Nova Science) p 29
- [17] Schilling J S and Klotz S 1992 *Physical Properties of High Temperature Superconductors* vol 3, ed D M Ginsberg (Singapore: World Scientific) p 59
- [18] Takahashi H and Mori N 1996 *Studies of High Temperature Superconductors* vol 16, ed A V Narlikar (New York: Nova Science) p 1
- [19] Zhou J-S, Goodenough J B, Sato H and Naito M 1999 *Phys. Rev. B* **59** 3827
- [20] Locquet J-P, Perret J, Seo J W and Fompeyrine J 1998 Superconducting and related oxides: physics and nanoengineering III *Proc. SPIE* **3481** 248
- [21] Bozovic I, Logvenov G, Belca I, Narimbetov B and Sveklo I 2002 *Phys. Rev. Lett.* **89** 107001